In

Metallurgical Applications of Shock-Wave and High-Strain-Rate Phenomena

Edited by

Lawrence E. Murr
Oregon Graduate Center
Beaverton, Oregon

Karl P. Staudhammer
Los Alamos National Laboratory
Los Alamos, New Mexico

Marc A. Meyers
New Mexico Institute of
Mining and Technology
Socorro, New Mexico

MARCEL DEKKER, INC. New York and Basel
1986

46

Effect of Metallurgical Parameters on Dynamic Fracture by Spalling of Copper

SAMUEL CHRISTY, HAN-RYONG PAK and MARC A. MEYERS

Center for Explosives Technology Research and
Department of Metallurgical and Materials Engineering
New Mexico Institute of Mining and Technology
Socorro, New Mexico 87801

The objective of this research program was to determine the effect of metallurgical parameters on the development of dynamic fracture by a tensile pulse in OFHC copper. Spalling was produced by explosive experiments. Copper specimens with varying grain sizes (250 μm, 90 μm, and 20 μm), in the predeformed condition (by rolling), and with two degrees of purity (99.99 and 99.5 pct) were subjected to impact pressures of 3.0, 3.5, and 3.8 GPa, at a constant initial pulse duration of 2.8 μs. The void volume fraction was determined in the recovered copper specimens as a function of distance from the impact surface. It was found to increase significantly between 3.0 and 3.8 GPa impact pressure. The metallurgical condition (grain size, predeformation, and impurity content) was found to have a marked effect on the spall strength of copper. The relative spall resistance of the various specimens did not correspond to their microhardnesses, since different metallurgical conditions exhibited different nucleation sites. While the large and medium-grain annealed specimens exhibited intergranular spalling, the small-grain and rolled specimens exhibited transgranular spalling. The primary nucleation sites for large and medium-grain specimens were grain boundaries, while grain interiors were important for the small-grain predeformed specimens. In specimens with low purity (99.5 pct), second-phase particles were the main nucleation sites.

It was possible to identify a void by high-voltage electron microscopy; this is the first report of the observation of a void formed by a tensile pulse. The void was found to be surrounded by a high density of dislocations.

I. INTRODUCTION

In 1914, Hopkinson [1], investigating the effect of explosives on metals, observed a very interesting phenomenon, which has since been termed Hopkinson fracture, scabbing, spalling, or spall fracture. A spall is a material failure produced by the action of tensile stress pulses developed in the interior of a solid body. Spalling may result from impact, detonation of contacting explosive, contact with electrically-exploded wire foil, deposition of intense pulses of radiation produced by electron beam accelerators or lasers. Spalling is important in military applications (armor penetration and fragmentation). A comprehensive review of spalling has been written by Meyers and Aimone [2]. From this review, it is clear that the effects of metallurgical parameters on spalling have only been superficially investigated, with the exception of the work of Jones and Dawson [3]. Additionally, only two mechanisms for void growth have been proposed [2,4] and no experimental verification has been obtained. Thus, the primary objectives of the investigation whose results are reported herein were:

1) to determine the effects of metallurgical parameters on the spalling behavior of a simple model material.

2) to observe a void by transmission electron microscopy in order to understand the micromechanical growth process.

II. EXPERIMENTAL TECHNIQUE

OFHC copper with 99.99% purity was chosen as a material for this investigation, since heterogeneous nucleation at second-phase particles can be avoided, because of its relative purity. This material was fully characterized by optical and electron microscopy to check for any pre-existing inhomogeneities prior to heat treatment. An electron microprobe analysis, to detect the presence of any kind of impurities, was performed. The results obtained indicated that the OFHC copper was a single phase, pure material. Metallographic examination of this material further proved the absence of inclusions or second phase particles.

OFHC copper was cold rolled to a 80% reduction in thickness. Three annealing treatments were selected in order to obtain a wide range of grain sizes. The target specimens were packed in SEN-PAK heat treating containers and annealed at the selected temperatures; the grain sizes were determined by the linear intercept method. A 400°C anneal for one hour yielded a 20 ± 3 μm grain intercept; a 800°C anneal for one hour yielded a 90 ± 8 μm grain intercept; a 840°C anneal for 36 hours yielded a 250 ± 20 μm grain intercept.

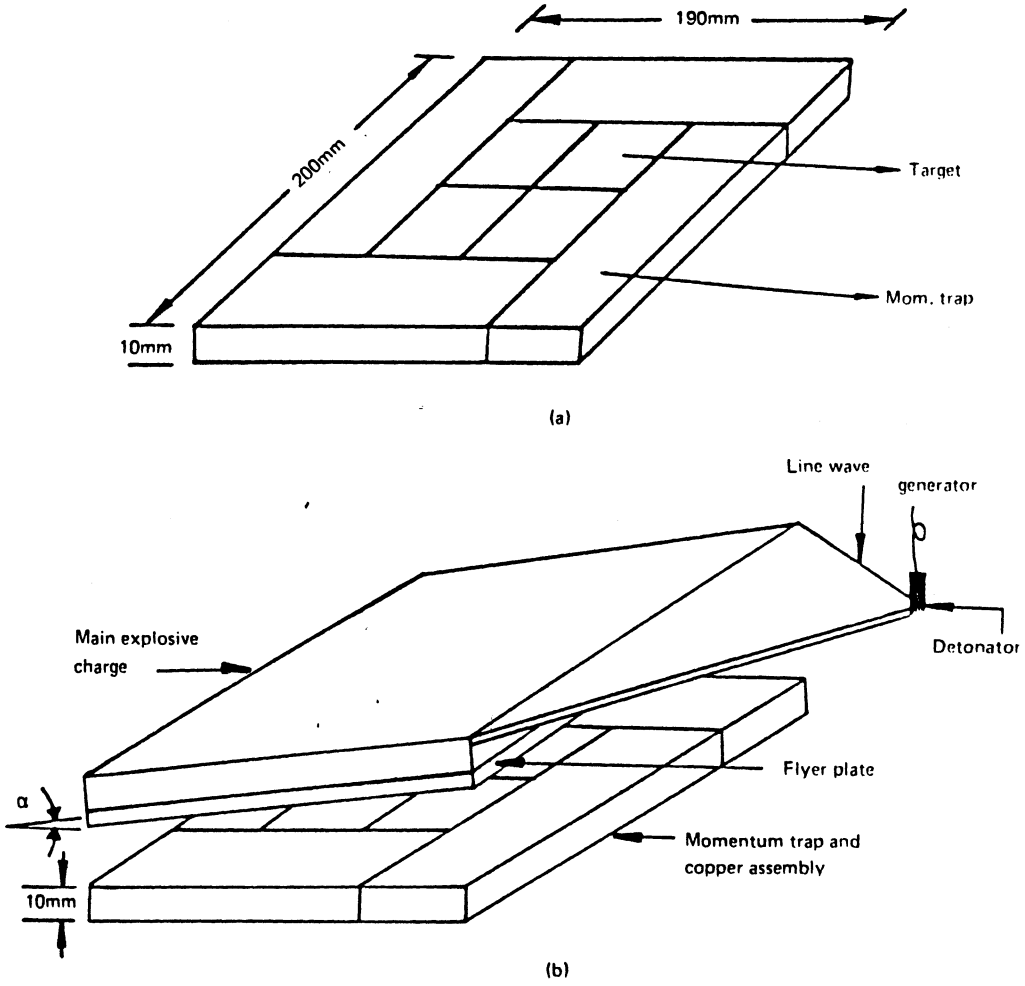

FIG. 1 *(a) Assembly of four copper specimens and lateral momentum traps. (b) Inclined plate set-up for accelerating flyer plate into targets.*

The spalling experiments were done by accelerating explosively-driven flyer plates onto targets. The flyer plates had a thickness of 5.25 mm, half of that of the targets: 10.50 mm. This ensured a maximum tensile pulse in the central region of the targets. Four specimens, representing the four metallurgical conditions (three different grain sizes and cold rolled copper) were mounted side-by-side, as shown in Fig. 1(a). They had dimensions of 45 x 50 x 10.5 mm and were precision machined to avoid gaps between the lateral surfaces. The four specimens were surrounded by four lateral momentum traps; these were made of copper plates with purity of 99.5%. This material contained a considerable amount of second-phase particles.

The flyer plate used to impact the target was accelerated by commercially available Detasheet explosive (having varying thicknesses to achieve the desired pressures), with an inclined plate assembly [Fig. 1(b)]. A rubber pad along with a thin sheet of cork was placed between the flyer plate and the explosive to avoid spallation of the flyer plate. One cannot achieve desired pulse durations if the flyer plate is spalled. The mass of the rubber pad and of the cork was added to the mass of the flyer plates in the computations. A detailed description of line-wave generators is given by Benedick [5] and of the inclined flyer-plate technique by DeCarli and Meyers [6].

The characteristics of the spall fracture were analyzed with optical and electron microscopy techniques. For optical microscopy the specimens were first mechanically polished using conventional methods. The etching was done with 5% ferric chloride, 15% hydrochloric acid and 80% ethanol for 30 - 40 seconds. Optical microscopy on the recovered specimens was performed on a Nikon Epiphot optical microscope.

Electron microscopy was performed on a Hitachi Perkin Elmer model HHS-2R scanning electron microscope and HU-200F Hitachi transmission electron microscope. Thin foils were prepared for transmission electron microscopy by sectioning the area away from and near the spall plane. The Fischione jet technique was used after thinning down the specimens to 150 μm. The electrolyte used was 67% methanol and 33% nitric acid. Thin foils were prepared at a voltage between 10-20 DC volts around -40°C.

Quantitative metallography was performed to compute the origin of nucleation sites for voids. Approximately ten micrographs were taken in the cross-sections of etched specimens at various magnifications with a Nikon Epiphot optical microscope. Individual voids nucleating at grain boundaries, within the grain, and at twin boundaries were counted for each specimen.

The procedure used to make a quantitative assessment of the extent of fracture damage in impacted plate specimens was to measure the individual microfractures on cross sections of the polished specimens. A series of micrographs was taken on the cross-sections of each impacted specimen, and each series was divided into ten sections. The surface area of individual microfractures was measured for each section with a digital planimeter (Calcomp 9000). This area of microfracture was then divided by the whole surface area of that section to obtain the volume fraction of spall.

The major goal of this proposed program was to study the mechanism for homogeneous void nucleation and void growth. The growth of microvoids is thought to occur by dislocation generation and movement. This required

the observation of dislocation arrangements in the vicinity of the voids. Transmission electron microscopy is the only tool available to observe such features. An HU-200F Hitachi transmission electron microscope was used to observe voids of a sub-micrometer size range. However, in the case of this 200 KV microscope the foil thickness is limited to only 0.2 μm(max) which makes it very difficult for the sub-micrometer voids to be observed. The density of these microvoids is not very high and if specimens with a larger foil thickness are used, there is an increased probability of the voids being observed. For this purpose high-voltage transmission electron microscopy (1500 KV) was used to observe thicker foils. The main advantage of using this technique is the ability to penetrate materials of truly representative thicknesses, and therefore improve the statistical significance of the data obtained. Other advantages are increased accuracy of electron diffraction and sharpness of detail in aperture dark-field images. This high-voltage transmission electron microscopy was conducted on the KRATOS EM 1500, at the National Center for Electron Microscopy, in Berkeley, California.

III. RESULTS AND DISCUSSION

Pressures and pulse duration were calculated from the impact velocities and flyer plate thickness, respectively, according to standard techniques. The tensile stresses were chosen such as to result in varying degrees of spalling. The basis for this was given by Davison and Graham [7], who report the spall strengths of copper varying between 2.3 and 0.6 GPa, in the 0.4-1.6 μs pulse duration range. It is now known, after work of Barbee et al. [8], Seaman, Curran, and Shockey [9,10] and Davison and Stevens [11], that spalling is a nucleation and growth (of crack or voids) process, and that it is a function of both tensile stress and stress duration. Thus, the spall strength is the tensile stress required for spalling, at a specific pulse duration. In the present study, the calculated initial tensile stress duration was 2.8 μs. Applying the calculations described by DeCarli and Meyers [6], explosive thicknesses of 6, 7, and 8 mm yielded pressures of 3, 3.5, and 3.8 GPa. These pressures and duration are slightly higher than the spall strengths given by Davison and Graham [7]. Davison and Graham [7] defined the spall strength at the first observations of voids, and not complete separation.

A. METALLOGRAPHIC OBSERVATIONS

The four pieces (large, medium, small, and as-rolled) were sectioned into two halves each. Figure 2 shows the cross-sections of large grains, medium

FIG. 2 *Cross-sectional view of large, medium, and small grained and rolled copper specimens impacted at 3.8 GPa pressure.*

grain, small grain and as-rolled specimens impacted at 3.8 GPa. The metallographic observations, microhardness measurements and quantitative assessments were performed on these cross-sections. One can notice that the spall damage is greatly dependent on the metallurgical condition of the specimen. The large grain sized specimens exhibit the greatest amount of spalling.

Considerable spall damage occurred in momentum traps placed on the lateral sides of the OFHC copper target pieces. Although the momentum traps were provided for the purpose of preventing lateral release waves from entering into the targets, it was decided to perform metallographic observations on the recovered momentum traps (99.5% Cu) also. This would help in studying the effect of second phase particles on spall fracture. Henceforth, in the results described in the following subsections, observational comparisons are made with respect to large grained, medium grained, small grained, as-rolled, and momentum trap specimens. The portion of the momentum traps adjacent to the internal interface with the specimens experienced essentially the same stress history as the specimens and was free of unwanted reflections.

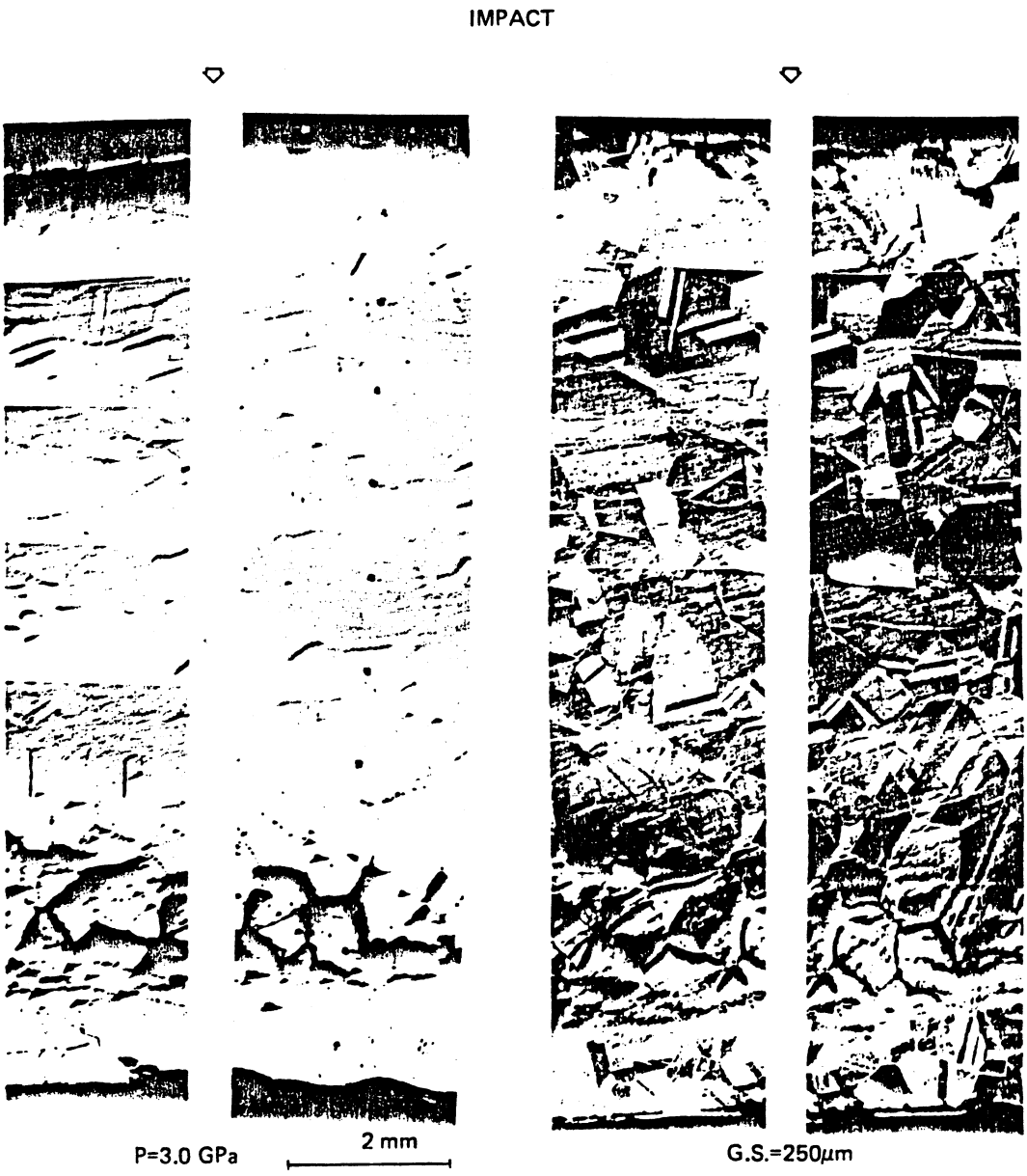

FIG. 3 *Cross-sectional view of large grained copper specimen impacted at 3.0 GPa pressure.*

Figures 3, 4 and 5 are a series of micrographs of cross-sections, across the thickness of the larged grained specimens, at 3.0, 3.5, and 3.8 GPa, respectively. The micrographs on the left hand side of each figure were taken in the as-polished condition, while the micrographs on the right hand side correspond to the same area and magnification after etching. The

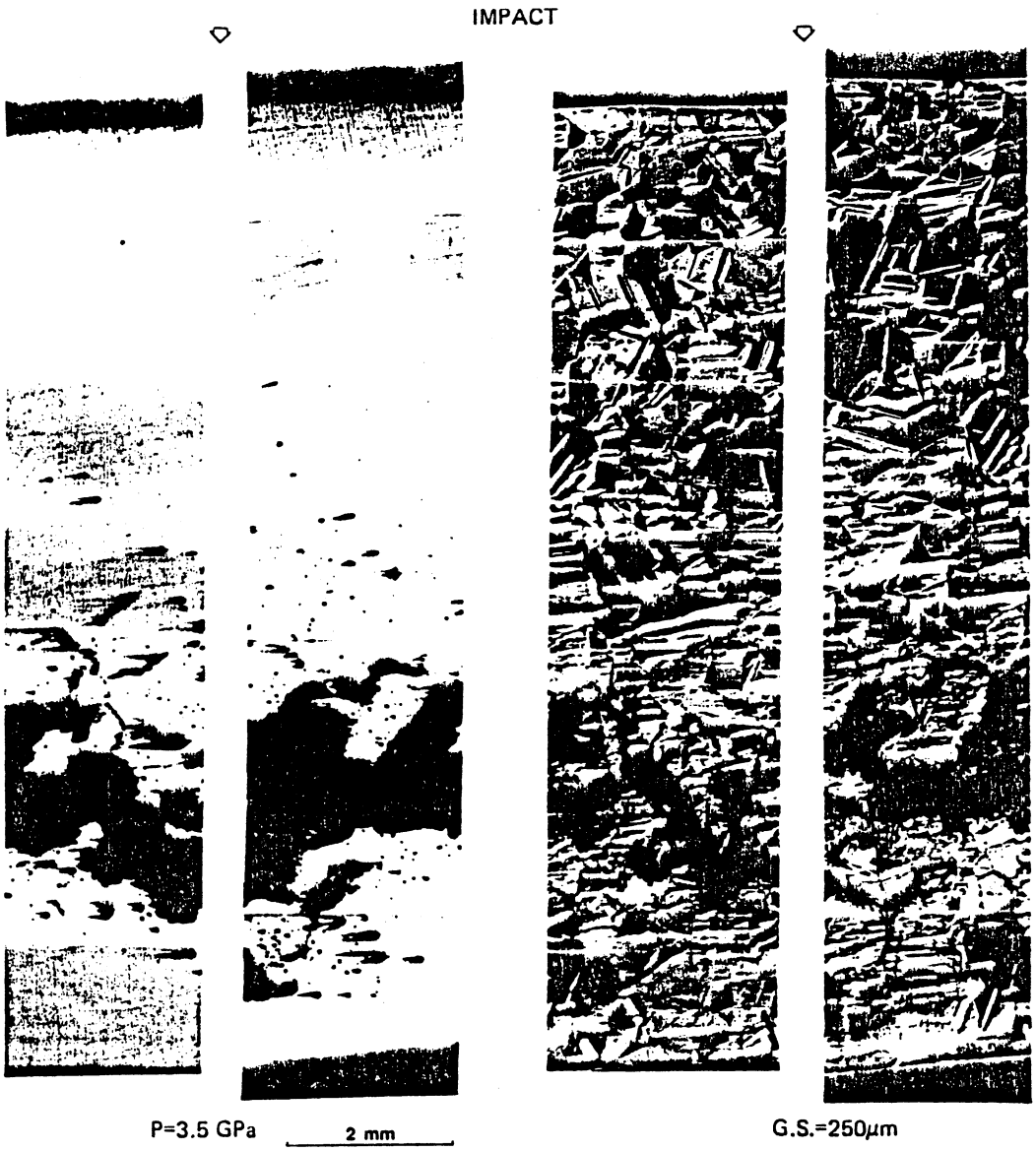

FIG. 4 *Cross-sectional view of large grained copper specimen impacted at 3.5 GPa pressure.*

same procedure was used for the other conditions. It can be clearly seen that impact damage increases with pressure (and the attendant tensile stress). The fracture is clearly intercrystalline. Closer examination of these micrographs shows grain boundaries as dominant nucleation sites. The microfracture is observed to have a range of shapes from spherical

FIG. 5 *Cross-sectional view of large grained copper specimen impacted at 3.8 GPa pressure.*

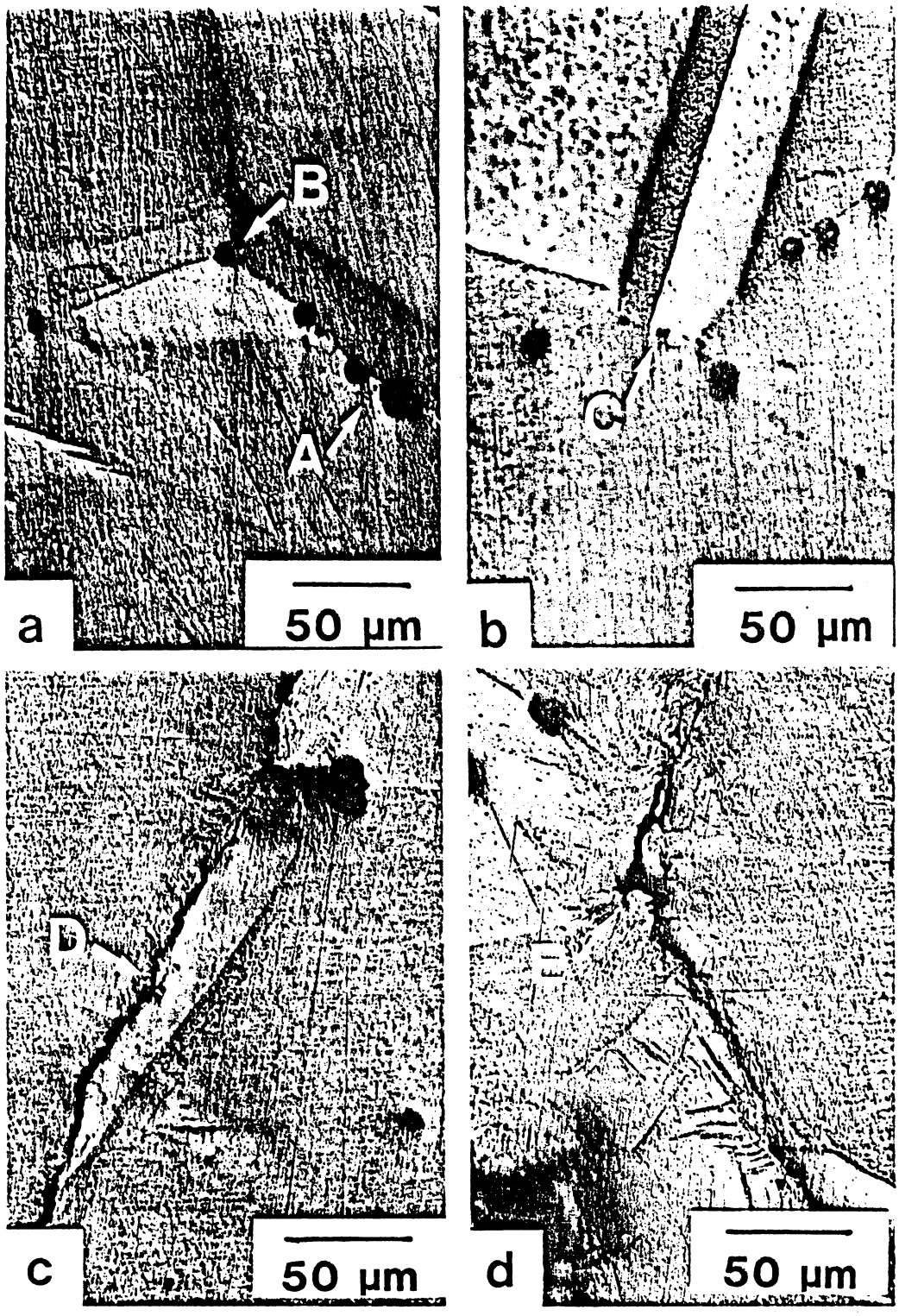

FIG. 6 *(a) and (b) nucleation of spherical voids at grain boundary, grain boundary triple point and the junction of grain boundary and twin; (c) and (d) plastic deformation bands along boundaries.*

voids to grain-boundary separation. In general, fracture damage did not appear exactly in the center of the target, but closer to the back free surface. The extent of damage was observed to increase with an increase in the impact pressure in all cases, irrespective of grain size and prior material treatment.

Figure 6 shows the distinguishing features of spalling in large grained copper. Figures 6(a) and 6(b) show spherical voids nucleated at a grain boundary (arrow 'A'), grain-boundary triple point (arrow 'B'), and the junction of a grain boundary and an annealing twin (arrow 'C'). Plastic deformation bands along the grain boundaries were observed as shown by arrows 'D' and 'E' in Fig. 6(c) and 6(d). These plastic deformation bands act as preferential nucleation sites for voids. When all voids have coalesced, the fracture is complete and appears as a planar crack. Hence, the fracture mode can be described as ductile intergranular. This term is introduced here to describe the unique morphology of the fracture surface: ductile, because it occurs by void growth, and intergranular, because it occurs along grain boundaries.

In general, plastic deformation in the form of twinning was also observed in large grained specimens. This feature is illustrated by the transmission electron micrograph in Fig. 7, which shows the presence of well formed deformation twins. One can see the offset between bend contours, which is indicative of twinning, because it shows that the region within the twin has a different crystallographic orientation. Small grain size specimens, on the other hand, do not exhibit such features. Similar results were obtained by Murr [12]. He was able to explain the occurrence of twinning in molybdenum by showing that, at a certain pressure, large grain sized specimens twinned more readily than small grain sized ones. This feature is not unique to shock loading, and has been observed in conventionally deformed Fe-3% Si [13].

Figures 8(a) to 8(d) are the micrographs of voids in the medium grain sample showing different morphologies. Figure 8(a) shows initiation of spherical voids at an annealing twin (marked by arrow). Figure 8(b) shows two square voids 'B' and 'C' with 'B' at the grain boundary, and 'C' in the interior of the grain. This observation seems to indicate the anisotropy of plastic deformation of pure copper. If the flow stresses were isotropic, the resultant void would be of spherical shape in order to minimize deformation and surface energy. Similar features were also observed in a nickel specimen by Meyers and Aimone [2] and an aluminum by Stevens et al. [4]. However, the occurrence of geometrical (square, rectangular, triangular) voids was less pronounced in copper than in nickel.

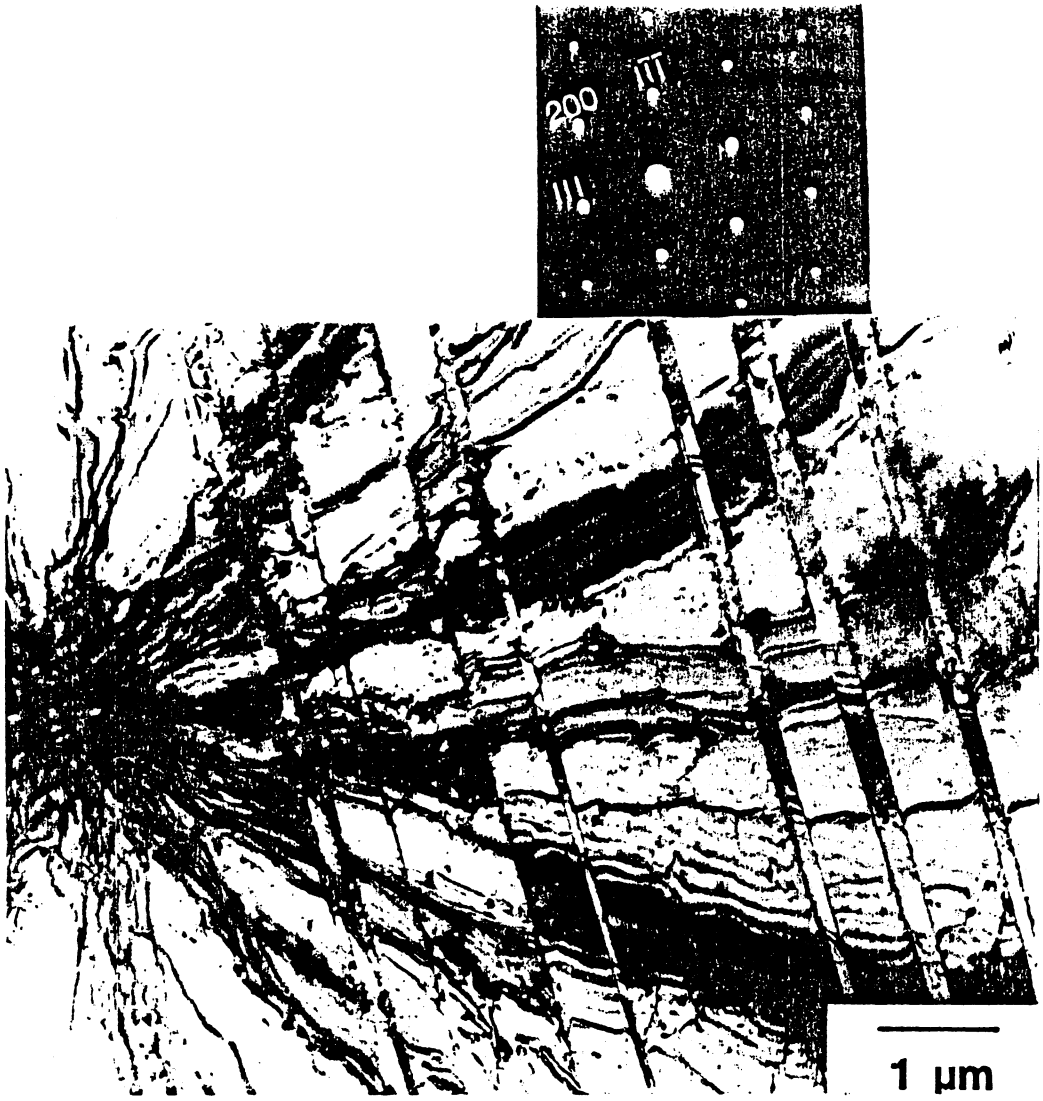

FIG. 7 *Transmission electron micrograph showing well formed deformation twins in large copper specimen impacted at 3.5 GPa pressure.*

Figure 8(c) shows a micrograph of a typical grain boundary distortion resulting from shear along the grain boundaries (arrow 'D'). The fracture in this case occurs by the shearing action between the two neighboring grains. Another feature of interest in this micrograph is the nucleation of a microvoid within the deformation band indicated by an arrow 'E'. Figure 8(d) also shows plastic localization in the form of a shear band. One can also see the severely deformed grain boundary.

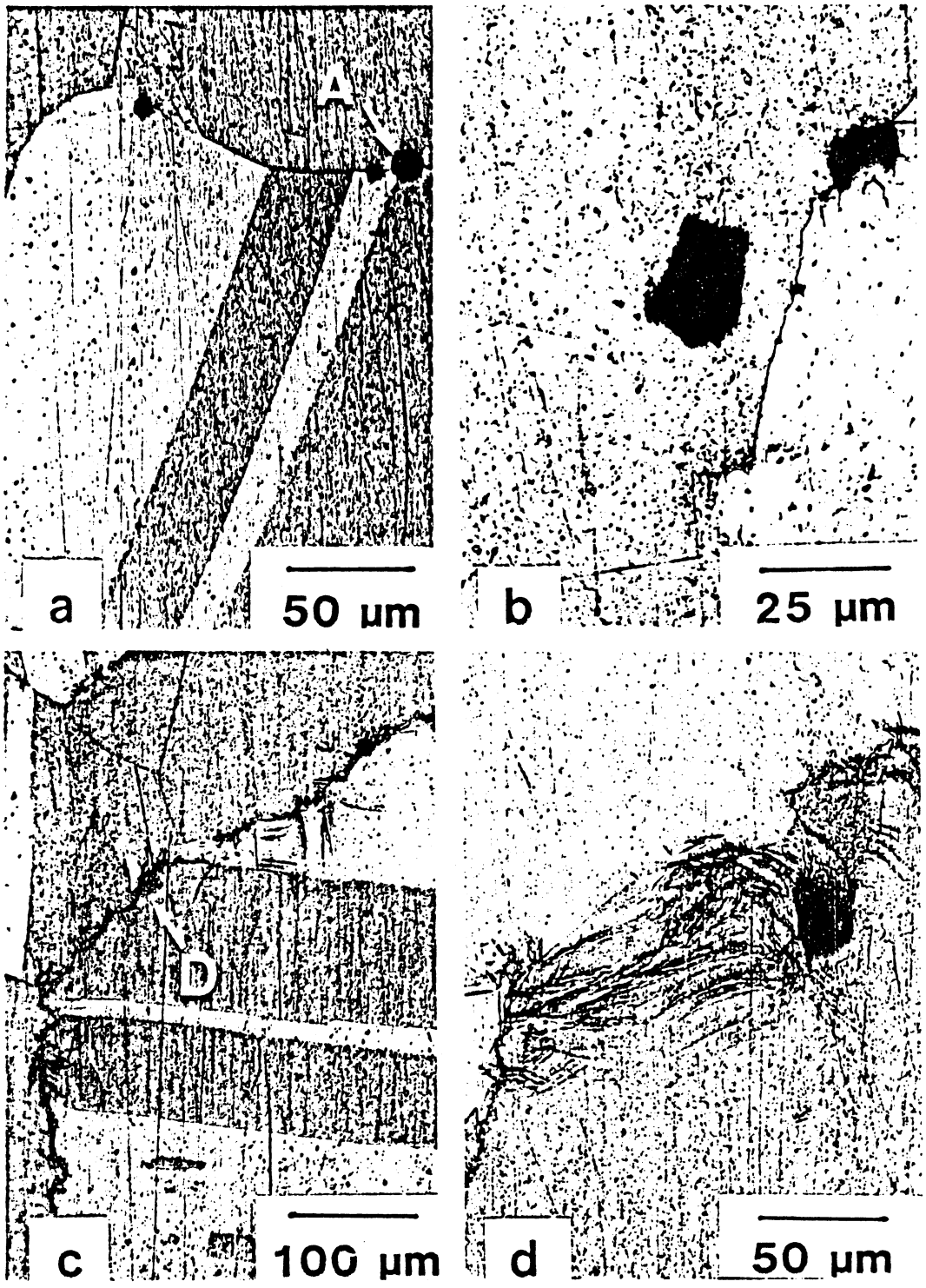

FIG. 8 *Optical micrographs of medium grained copper specimen showing (a) nucleation of spherical voids at annealing twins, (b) roughly square voids, (c) and (d) grain boundary sliding.*

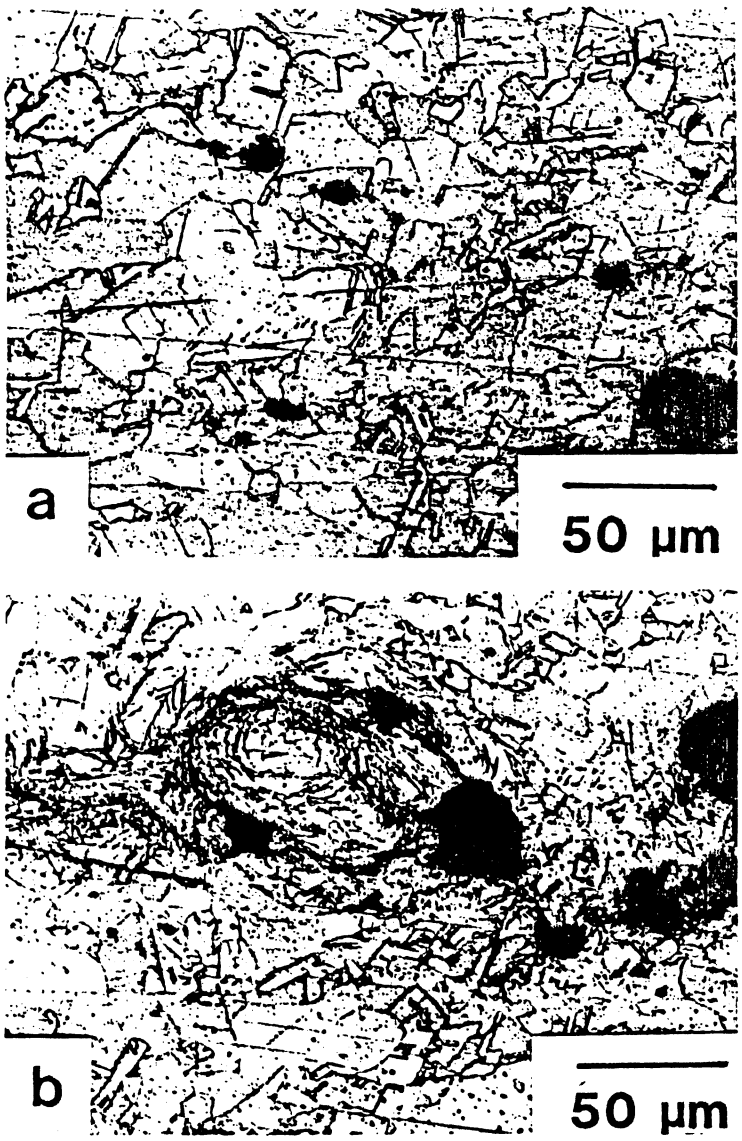

FIG. 9 *(a) Optical micrographs of small grained copper specimen impacted at 3.8 GPa pressure showing the nucleation of voids inside the grains; (b) the link-up of individual microfractures through deformation bands.*

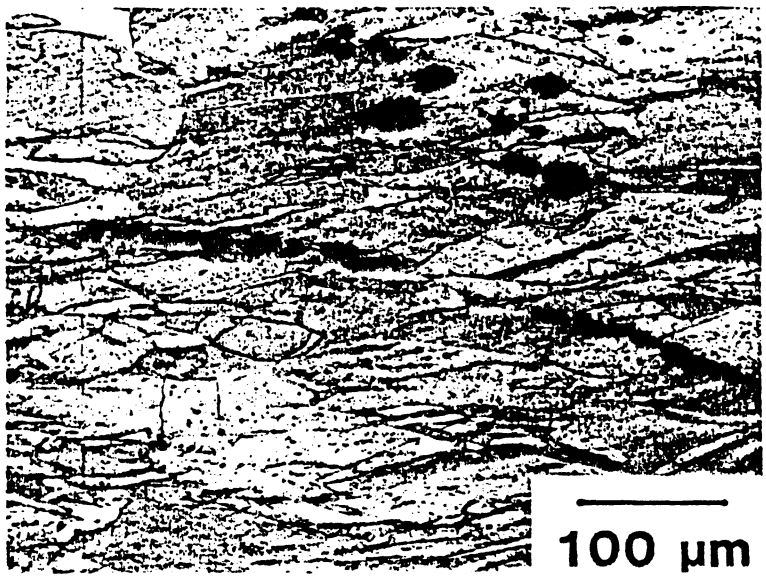

FIG. 10 *Optical micrograph of rolled copper specimen showing void groups aligned in the direction of rolling.*

Figure 9(a) is a micrograph of small grained copper specimen impacted at 3.8 GPa pressure. It can be seen that numerous spherical voids were found to be nucleated inside the grains and not at the grain boundaries, in contrast with the large and medium grain annealed copper specimens. Plastic deformation in the form of bands was also observed in the small grained specimens. A typical example can be seen in Fig. 9(b). Plastic flow between voids can be seen.

Figure 10 shows the typical spall damage produced in the as-rolled copper. One can see numerous spherical voids within the elongated grains. It can be seen that most voids nucleate inside the grains (and not at the grain boundaries), in contrast with the large and medium grain annealed specimens. Plastic deformation by rolling seems to decrease the propensity of the grain boundaries to act as nucleation sites.

Figure 11 shows a series of micrographs taken at the cross-section of the momentum trap (copper with 0.5% impurities) after the 3.0 GPa spall experiment. These micrographs show the distribution of microfractures. Spalling occurs by the production of parallel layers of voids. This flaked spall is readily understood by looking at the distribution of second-phase particles. These are aligned as "stringers" and they are nucleation sites for voids.

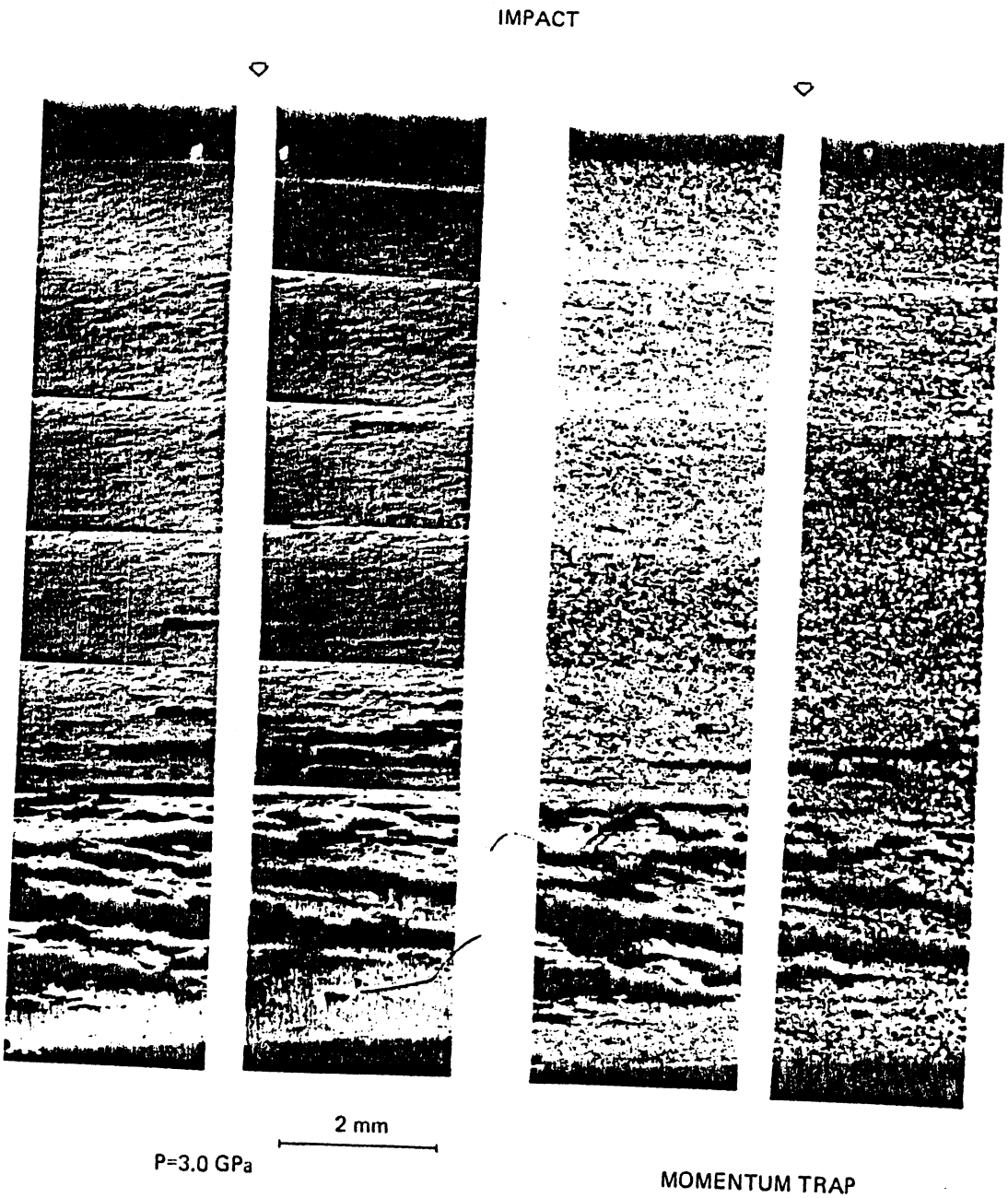

FIG. 11 *Cross-sectional view of momentum trap specimen impacted at 3.0 GPa pressure.*

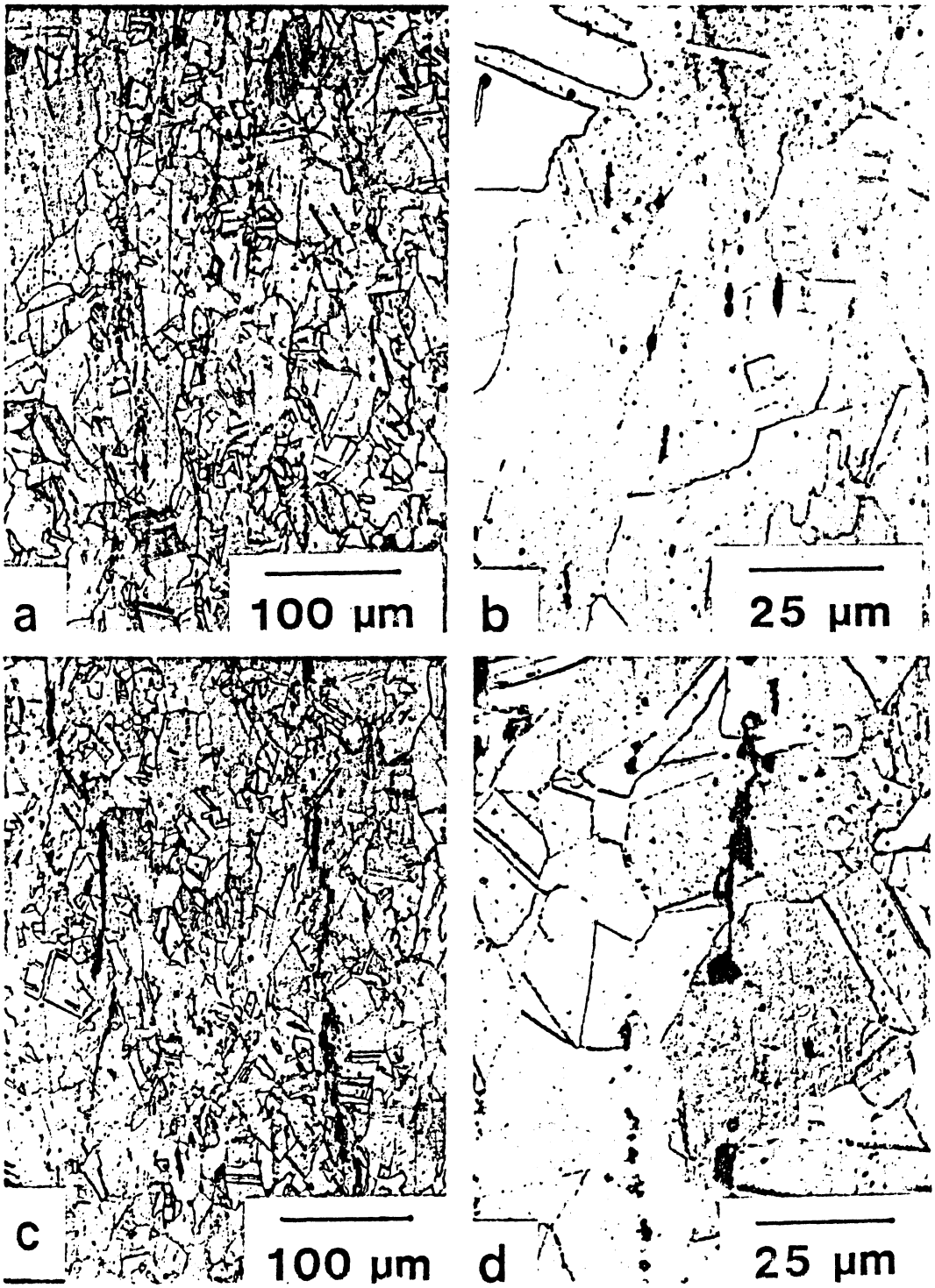

FIG. 12 *Optical micrographs of momentum trap copper specimens showing (a) distribution of second-phase particles (b) nucleation of void at second-phase particles (c) string of voids (d) void nucleation, growth and coalescence at fractured particles.*

Figure 12(a) shows the distribution of second phase particles, which are readily available nucleation sites for microfractures. Figure 12(b) shows a configuration of voids associated with an array of second phase particles. One sees a sharp microcrack at the edge of a spherical void as indicated by arrow 'A'. Arrow 'B' shows the coalescence of neighboring voids through a sharp crack. Figure 12(c) shows a string of fractured inclusions (indicated by arrows), most of which nucleated a void. As they grow and coalesce with other voids, they become elongated in the direction of the inclusion. Figure 12(d), taken at higher magnification, shows a complete event of microfracturing starting from a fractured particle at 'A', the nucleation of void at 'B', and coalescence of neighboring voids at 'C'. One can also see irregular-shaped voids within the second phase particles, which can be termed as microcracks. This is indicated by arrow 'D'. At lower magnification the original particles cannot be identified, as they are all taken up by growing voids. These observations of spalling in the momentum trap can be described by the interaction of tensile waves with second phase particles. Under the influence of a tensile pulse of sufficient magnitude, brittle second phase particles are fractured, and voids are nucleated. Void growth and coalescence then occur as successive steps in producing a spall surface.

B. FRACTOGRAPHIC OBSERVATIONS

Copper is a very ductile material and both quasistatic and dynamic fractures show a characteristic dimpled appearance. Scanning electron microscopic examination of the fracture surfaces of large and medium grained copper specimens, impacted at 3.8 GPa pressure, revealed a consistent ductile intergranular fracture mode as indicated by the presence of dimple failure along grain boundaries in the micrographs in Fig. 13. One can also see the uniform spallation of individual grains in both large and medium grained copper specimens. It is apparent, on examining Figs. 13(a) and 13(b), that microstructural features associated with the grain boundaries do influence dynamic fracture behavior.

Figures 13(c) and (d) are micrographs taken on the fracture surfaces of small grained and rolled copper specimens, respectively. These fractographs reveal the transgranular ductile fracture mode, since large numbers of voids are nucleated within the grains. The momentum trap, on the other hand, exhibited heterogeneous nucleation at second-phase particles. A typical example of microvoid nucleation by fracture of brittle second-phase particles is shown in the micrographs in Figs. 14(a) and (b). Quasistatic

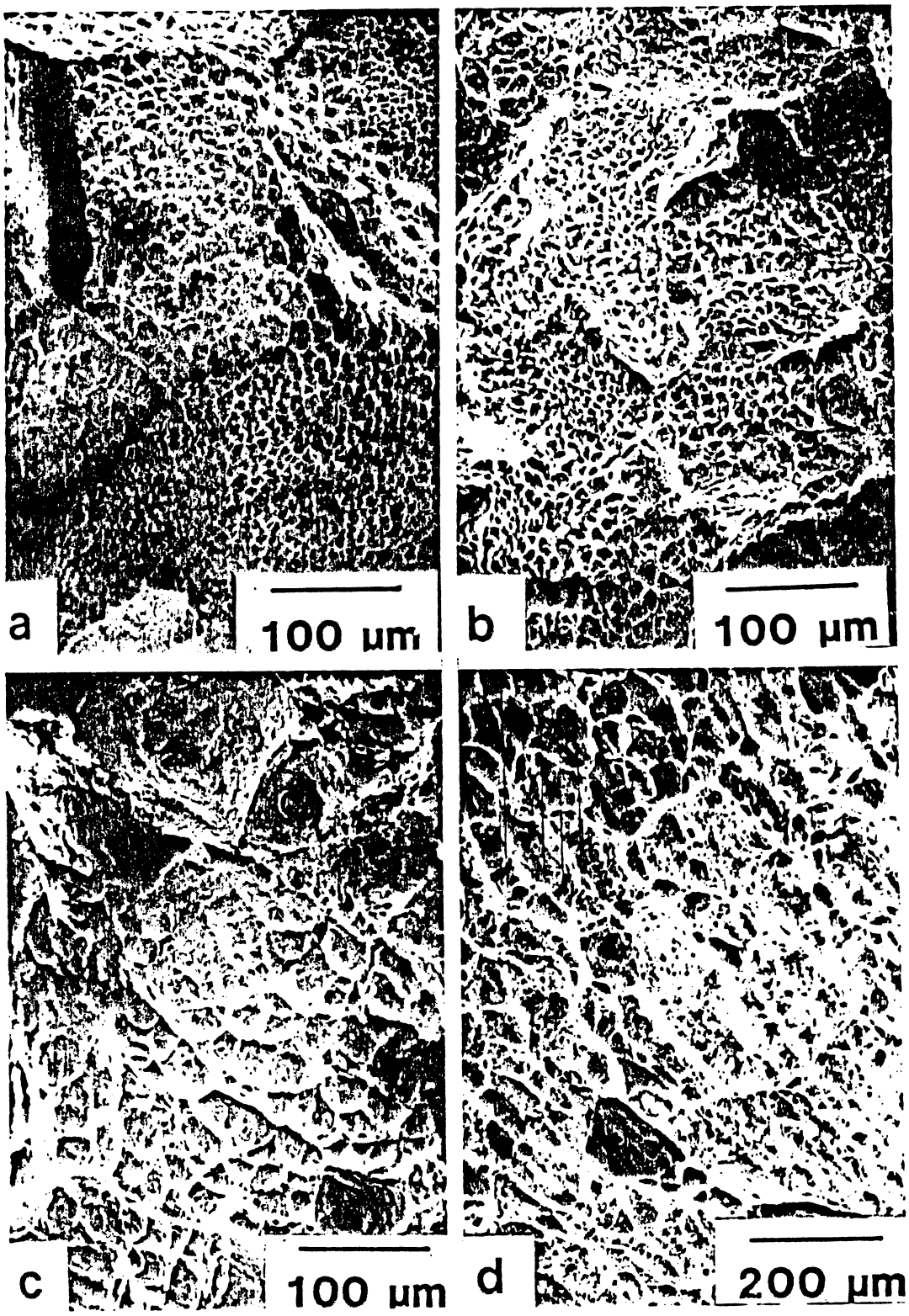

FIG. 13 *Fractographs of (a) large and (b) medium grained copper specimens impacted at 3.8 GPa pressure showing ductile intergranular fracture mode. Fractographs of (c) small grained and (d) rolled copper specimens showing transgranular dimple mode.*

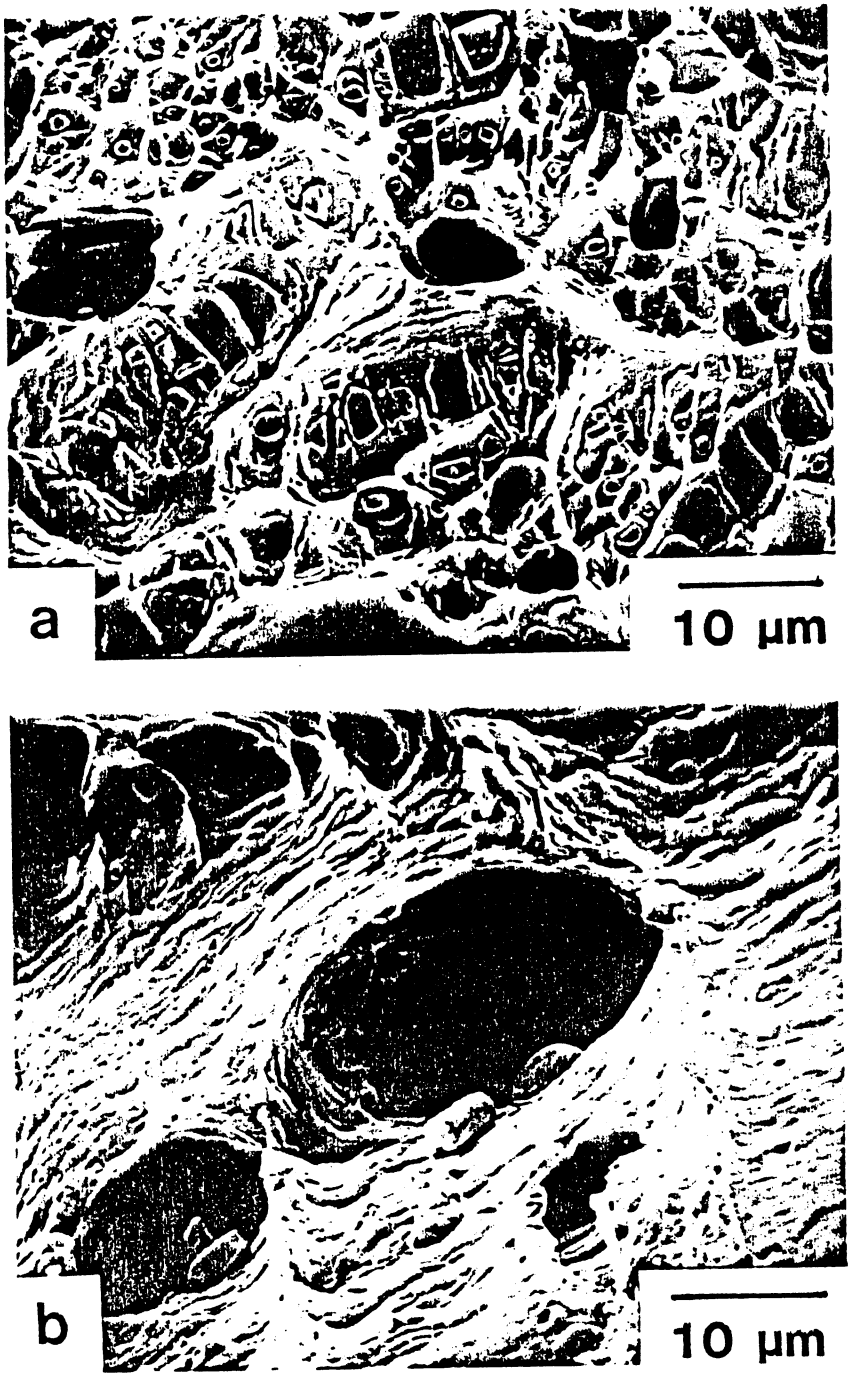

FIG. 14 *Fractographs (a) and (b) of momentum trap copper specimen showing heterogeneous nucleation of voids at second-phase particles.*

tensile tests at a nominal velocity of 0.01mm/sec were conducted using a MTS tensile testing machine on small grained and large grained copper specimens at room temperature. The fracture surfaces of tensile specimens were examined, in order to compare their quasistatic and dynamic fracture behavior. From these fractographic observations it appears that the intergranular fracture mode observed in shock loaded copper is not evident in copper tested under quasistatic loading conditions.

C. MEASUREMENT OF VOID VOLUME FRACTION

The volume fraction of voids formed upon spalling was computed as a function of impact pressure as well as a function of different metallurgical conditions (large, medium, small, rolled and momentum trap). Figure 15(a) compares the extent of spall fracture in large grained copper specimens, as a function of impact pressure (3.0, 3.5, and 3.8 GPa). One notices that the amount of spall damage increases with increase in impact pressure. Figure 15(b) shows the variation of volume fraction of voids computed in large grain, medium grain, small grain, as-rolled, and momentum trap specimens subjected to a pressure of 3.0 GPa. It can be seen that the momentum trap has sustained the maximum amount of damage compared to large and medium-grain size copper. The rolled specimen, on the other hand, shows very little volume fraction of fracture. Small grained specimens do not show any damage at this stress level. This indicates that the small grainedspecimen exhibits superior dynamic fracture resistance compared to the other specimens. The momentum trap has a much higher density of second-phase particles and at this stress level a large number of these particles (heterogeneous sites) can be activated more rapidly than other nucleation sites (homogeneous) present in the large grained, medium grained, small grained, and rolled copper specimens.

Figure 15(c) compares the spall damage of different specimens impacted at 3.5 GPa pressure. The large grained specimen exhibits the heaviest damage. The rolled specimen, on the other hand, shows superior spall resistance. In the case of specimens impacted at 3.8 GPa pressure [Fig. 15(d)], the momentum trap, large grained and medium grained copper specimens show a higher amount of damage compared to small grained and rolled specimens. The position of the peaks corresponds to the position of the spall plane, where these materials may have experienced the first tensile pulse. As the metal spalls, the stress experienced by adjacent regions is reduced because of the release waves generated at the free surfaces.

Thus, the superiority of the small grained copper in dynamic experiments is similar to what one would expect from quasi-static failure

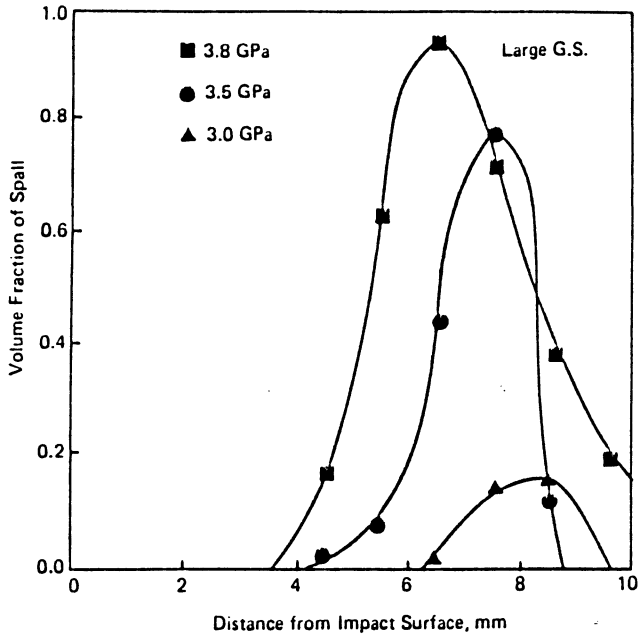

(a)

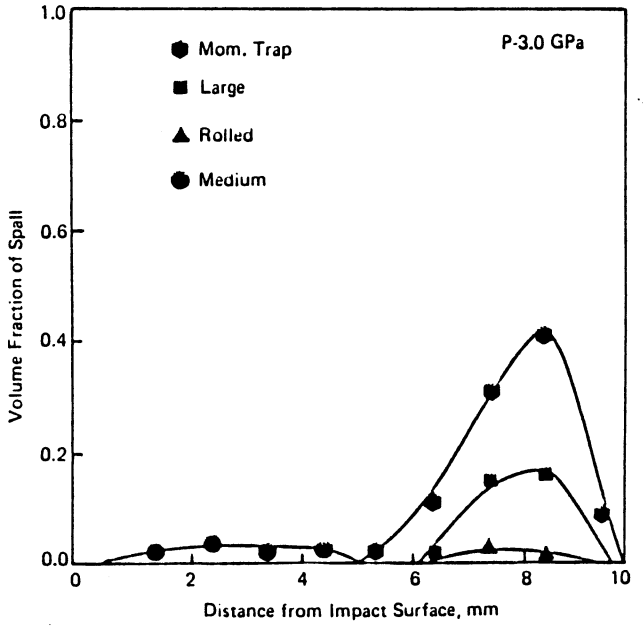

(b)

FIG. 15 *Volume fraction of voids formed upon spalling: (a) effect of pressure on large grain size specimens; all metallurgical conditions at (b) 3.0 GPa, (c) 3.5 GPa, and (d) 3.8 GPa.*

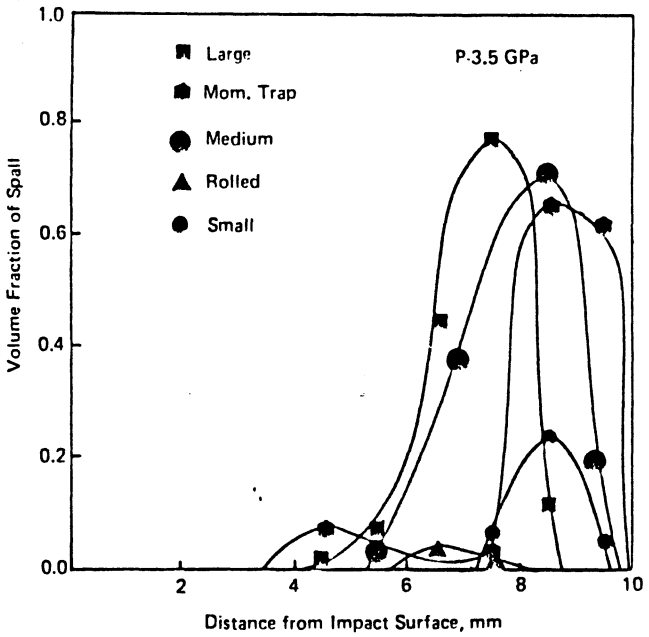
Large
Mom. Trap
Medium
Rolled
Small
P-3.5 GPa
Volume Fraction of Spall
1.0
0.8
0.6
0.4
0.2
0.0
2
4
6
8
10
Distance from Impact Surface, mm

(c)

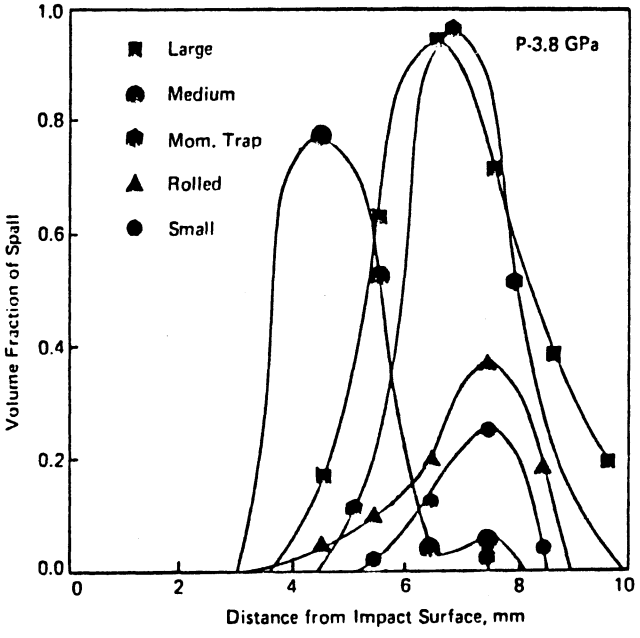
Large
Medium
Mom. Trap
Rolled
Small
P-3.8 GPa
Volume Fraction of Spall
1.0
0.8
0.6
0.4
0.2
0.0
0
2
4
6
8
10
Distance from Impact Surface, mm

(d)

TABLE 1 *Microhardness of five metallurgical conditions (HVN)*

	Before Shock	After Shock
Large Grain (250 μm)	*70*	*90*
Medium Grain (90 μm)	*87*	*87*
Small Grain (20 μm)	*95*	*90*
Rolled	*120*	*120*
Momentum trap (99.5%)	*98*	*110*

behavior. One important observation is that the spall strength of the copper is not directly related to hardness. The hardnesses before and after shocking for the five conditions are listed in Table 1. From these values, one would expect the rolled material to have the highest spall strength. However, the small-grained specimens, with a substantially lower hardness, exhibited a high spall strength. Thus, one can conclude that the dynamic spall resistance of copper does not correlate directly with the hardness. Spalling results from the nucleation, growth, and coalescence of voids. The momentum trap has an initial microhardness equivalent to the small grain specimen; nevertheless, it has a much lower resistance to spalling (comparable to the large grain specimens).

D. QUANTITATIVE ASSESSMENT OF VOID INITIATION SITES

Table 2 shows a quantitative computation of the number of void invitation sites in large grained, medium grained, small grained, and rolled copper specimens. In general, grain boundaries act as main initiation sites in the large and medium grained specimens. In large and medium grained specimens the number of voids nucleated at grain boundaries is much higher than in the small grained and rolled specimens. The failure process proceeds more rapidly with increasing stress in large grained specimens compared to others. This is due to the fact that a much higher concentration of initiation sites is present in large grained specimens, and a much larger number of these are activated under dynamic stress leading to intergranular fracture.

TABLE 2 *Quantitative assessment of microfractures (voids) in OFHA copper*

Material (OFHC Copper)	No. of voids at grain boundary	No. of voids at center of grain	No. of voids at twin boundary	Total voids counted
Large grained (250 μm)	*141*	*19*	*22*	*182*
	77%	*10%*	*12%*	
Medium grained (90 μm)	*50*	*18*	*9*	*77*
	65%	*28%*	*12%*	
Small grained (20 μm)	*43*	*80*	*18*	*141*
	30%	*56%*	*13%*	
Rolled	*77*	*79*	*0*	*156*
	49%	*51%*	*0%*	

E. HIGH-VOLTAGE TRANSMISSION ELECTRON MICROSCOPY OBSERVATIONS

It has been shown in previous sections that the density of voids produced by impact increased as the impact pressure and the grain size of the target materials increased. Two models have been proposed to explain the formation mechanism of such voids [2,4]. However, neither of them can explain the phenomenon very well. High-voltage transmission electron microscopy (1500 kV) was employed to obtain microstructural information on the voids produced by impact, which could explain the formation mechanism of these voids.

The identification of small voids is not a simple task because of their low concentration (density) and the difficulty of identification. Only one void could be positively identified, and this was possible by high-voltage transmission electron microscopy. Figure 16 shows a peanut-shaped void observed in a foil taken from small-grain sized copper subjected to an impact pressure of 3.8 GPa. The pair of stereo-micrographs in Fig. 17 unmistakenly identify the feature as a void located in the sample. The three-dimensional features can be observed using the appropriate viewing instrument. These micrographs illustrate an elongated void which is surrounded by a heavily dislocated area. The high density of dislocations around the void is thought to be produced by shear strains which are required for the growth of the microvoid during the application of the tensile pulse. A micromechanical model for void growth is being developed.

FIG. 16 *The peanut shaped void observed in a thin foil taken from small grained copper specimen subjected to a shock wave amplitude of 3.8 GPa.*

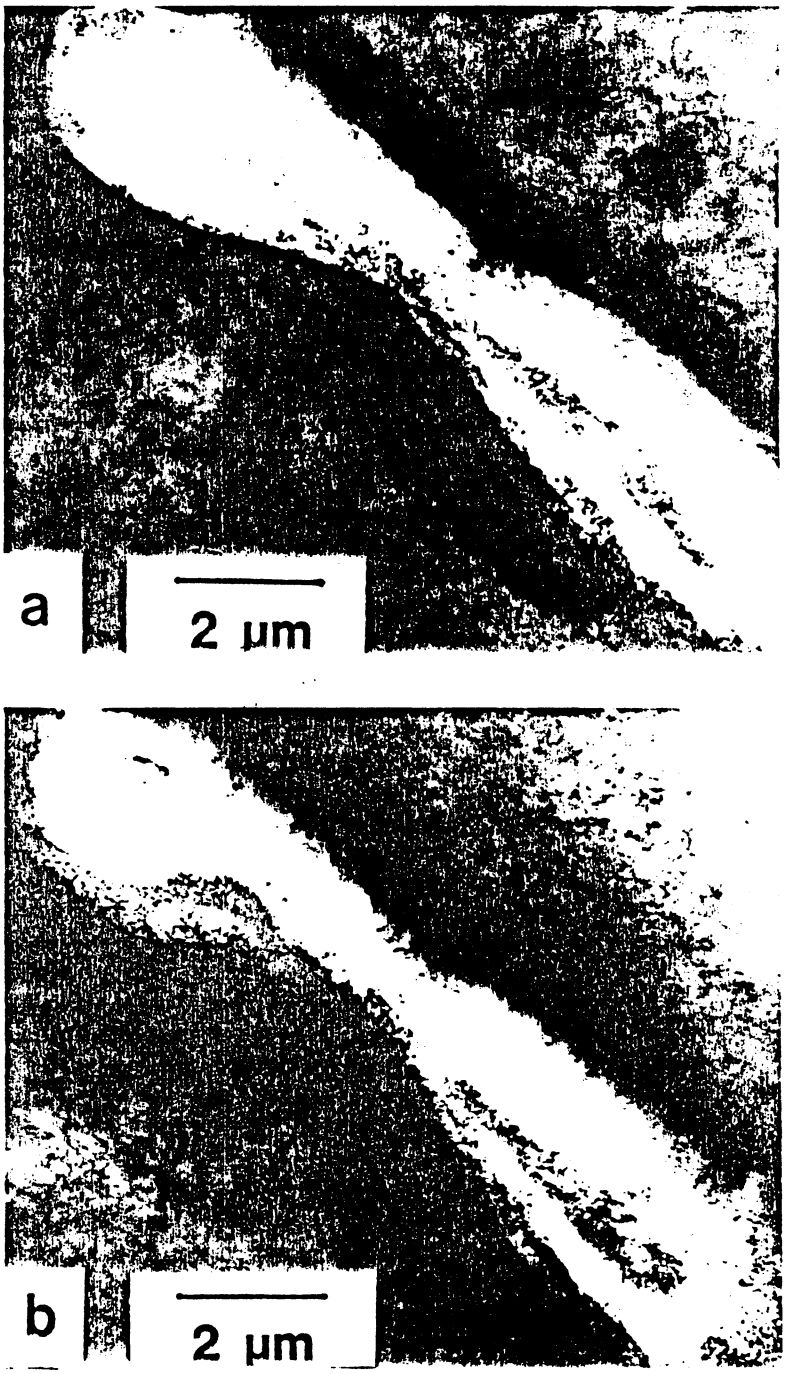

FIG. 17 *A pair of stereo micrographs of the small grained copper impacted at 3.8 GPa pressure, showing elongated void surrounded by high density of dislocations.*

IV. CONCLUSIONS

(1) It is shown that the tensile stresses produced in copper by the reflection of a shock wave at a free surface induce spalling which occurs as a process of nucleation, growth and coalescence of voids.

(2) Fractographic observations of copper specimens have shown that both quasistatic and dynamic fracture have a characteristic dimpled appearance. Large and medium grained copper specimens exhibit ductile intergranular fracture mode, whereas small grained and rolled copper specimens show a ductile transgranular fracture mode.

(3) Heterogeneous nucleation at second-phase particles was the most prevalent mechanism of spall initiation in the momentum trap copper specimens.

(4) Quantitative metallography results reveal that the amount of fracture increases with increase in impact pressure in OFHC copper. The various conditions, in order of increasing spall resistance are: large grain size (250 μm); medium grain size (90 μm); rolled; small grain size (20 μm).

(5) A peanut-shaped void surrounded by a highly dislocated region was observed in a small grain copper specimen impacted at 3.8 GPa pressure by high-voltage transmission electron microscopy. The high density of dislocations around the void is thought to be produced by shear strains which are required for the growth of the microvoid.

ACKNOWLEDGEMENT

Support for this research was provided by National Science Foundation Grant DMR 8115127 and the Center for Explosives Technology Research. Dr. A. D. Romig, Jr., Sandia National Laboratories, provided help with the electron microscope analysis of the copper. Dr. James Mote, University of Denver, is acknowledged for his help in rolling the copper plate. Mr. Dennis Hunter and Mr. J. Claffy, of TERA/NMIMT, assisted in the explosive experiments. The help of Dr. K. Westmacott and Mr. D. Akland, of the National Center for Electron Microscopy, is greatly appreciated.

REFERENCES

1. B. Hopkinson, *Trans. R. Soc. (Lond.) 213A:* 437 (1914).
2. M. A. Meyers and C. T. Aimone, *Prog. in Mat. Sci. 28:* 1 (1983).
3. W. B. Jones and H. I. Dawson, in *Metallurgical Effects at High Strain Rates,* R. W. Rohde, B. M. Butcher, J. R. Holland, and C. H. Karnes (eds.), Plenum Press, New York, 1973, p. 459.

4. A. L. Stevens, L. Davison, and W. E. Warren, *J. Appl. Phys. 43:* 4922 (1972).

5. W. B. Benedick, in *Behavior and Utilization of Explosives in Engineering Designs,* L. Davison, J. E. Kennedy, and F. Coffey (eds.), ASME, New Mexico, 1972, p. 47.

6. P. S. DeCarli and M. A. Meyers, in *Shock Waves and High-Strain-Rate Phenomena in Metals: Concepts and Applications,* M. A. Meyers and L. E. Murr (eds.), Plenum Press, New York, 1982, p. 341.

7. L. Davison and R. A. Graham, *Physics Reports, 55:* 257 (1979).

8. T. W. Barbee, L. Seaman, R. Crewdson, and D. R. Curran, *J. Mater. J.M.L.S.A. 7:* 393 (1972).

9. L. Seaman, D. A. Shockey, and D. R. Curran, in *Dynamic Crack Propagation,* G. C. Sih (ed.), Noordhoff, Leyden, 1973, p. 629.

10. D. R. Curran, L. Seaman, and D. A. Shockey, *Physics Today,* Jan. (1977), 46.

11. L. Davison and A. L. Stevens, *J. of Applied Physics 43:* 988 (1972).

12. L. E. Murr, in *Shock Waves and High-Strain-Rate Phenomena in Metals: Concepts and Applications,* Plenum Press, New York, 1981, p. 645.

13. M. J. Marcinkowski and H. A. Lipsitt, *Acta Met. 10:* 95 (1962).

ADDENDUM

At the 1985 EXPLOMET conference we were informed by Dr. Z. Rosenberg that a similar study on copper had been conducted and published by:

D.G. Brandon, M. Boas, and Z. Rosenberg, "Effect of Grain Boundaries on Ductile Fracture Under Planar Impact", in "Mechanical Properties at High Rates of Strain", 1984, The Institute of Physics, pp. 261-268.

The results of our (independent) investigation (S. Christy, "Dynamic Fracture by Spalling in Titanium and Copper", M.Sc. Thesis, New Mexico Institute of Mining and Technology, Socorro, New Mexico, October 1981) are in full agreement with these results. A "pseudo brittle" fracture growth process, identical to our "intergranular ductile mode" is described by Brandon, Boas, and Rosenberg. These investigators were, thus, the first to report on intergranular spall fracture in high-purity copper.